Journal of Applied Polymer Science

Expansion of Core–Shell PS/PMMA Particles

Odinei Hess Gonçalves,[1] Fernanda Vitória Leimann,[1] Pedro Henrique Hermes de Araújo,[2] Ricardo Antonio Francisco Machado[2]

[1]Post-Graduation Program of Food Technology, Federal University of Technology - Paraná, Campo Mourão, PR, Brazil
[2]BR 369, km 0, 5, Campo Mourão, 87301-006
Correspondence to: O. H. Gonçalves (E-mail: odinei@utfpr.edu.br)

ABSTRACT: Structured micrometric polystyrene/poly(methyl methacrylate) particles were obtained by suspension polymerization and their expansion behavior was investigated using *n*-pentane as blowing agent. The expanded particles presented two distinct microstructures with an outer region (PMMA-rich shell) composed by cells of about 10 μm while the center of the particle (PS-rich core) had much larger cells (50–100 μm). The core–shell particles did not expand at 100°C meaning that the PMMA shell hindered the expansion of the particles. Maximum expansion was dependent on the PMMA concentration and also on the heating temperature and the increase in the PMMA molar mass led to a delay in the onset of the process. © 2013 Wiley Periodicals, Inc. J. Appl. Polym. Sci. 130: 4521–4527, 2013

KEYWORDS: foams; thermoplastics; free radical polymerization

Received 8 August 2013; accepted 4 July 2013; Published online 24 July 2013
DOI: 10.1002/app.39731

INTRODUCTION

Plastic foams are two phase materials consisting of a solid continuous polymer matrix and a gas phase usually composed by blowing agent and air. A wide range of properties can be obtained as they are controlled by cell size distribution and also by the composition and concentration of the gas entrapped inside the polymer cells.[1] Excellent reviews on plastic foams and especially on expandable polystyrene (EPS) are available[2–5] and suspension polymerization is the process of choice to obtain expandable polymer beads. Seeded suspension polymerization is a modified approach in which a second monomer is polymerized on preformed particles yielding particles presenting improved mechanical or chemical properties.[6–9] The final molecular weight distribution and intra particle composition are dependent on a complex interplay between polymerization kinetics and monomer diffusion which is affected by process conditions and seed-monomer interactions.[10,11]

Large scale production of expandable polystyrene particles makes use of physical blowing agents consisting in low boiling point liquids like pentane isomers incorporated in the polystyrene (PS) particles during the polymerization reaction or in a subsequent step.[12,13] The study of the expansion process is not recent and was reported in both scientific and patent literature due to its importance to the industrial scale production of foam plastics.[14–19]

The increasing demand for materials with improved properties has been the driving force of the current researches on plastic foams. It is known that polystyrene presents low mechanical strength when compared to other thermoplastics and that it is readily soluble in most nonpolar solvents[20] restricting its application. Expandable poly(styrene-co-divinylbenzene) particles whose chemical composition varies along their radius were obtained by seeded polymerization presenting improved mechanical and thermal properties.[21,22] However, expansion was hindered by the formation of a reticulated network (gel) due to the reaction with divinylbenzene which may also makes recycling more difficult. The synthesis of poly(methyl methacrylate) (PMMA) foamed particles were recently investigated[23] since PMMA particles can also be obtained by suspension polymerization[24] and *n*-pentane can be used as blowing agent. Moreover, when compared to polystyrene, PMMA is more resistant to nonpolar solvents due to its carbonyl groups and presents higher impact strength.[25] Although the expandability of PMMA showed promising results, methyl methacrylate is more expensive than styrene leading to high production costs. The expansion of P(S-MMA) were also carried out using *n*-pentane as blowing agent[26–28] and the final expanded microstructure and density were affected by copolymer composition and process parameters. The researchers used a high amount of MMA which can still raise the cost of the material to a prohibitive level. One alternative would be to obtain foams composed by polystyrene containing low amounts of PMMA in order to improve properties without increasing the raw material costs. Complex morphology like core–shell particles could also be of interest because specific properties can be inserted using small amounts of the shell polymer.

The synthesis of core-shell PS/PMMA particles with sizes of about 1000 μm was described elsewhere[10,23] and it was confirmed that the particles presented a nonequilibrium morphology with a PS-rich core and a shell consisting of PMMA domains distributed in a PS matrix. Parameters like shell thickness and PMMA concentration were dependent on the synthesis procedure but the aforementioned literatures did not show any results on the expansion of the particles. The possibility of using these core–shell particles to obtain foamed materials could be of interest since it was demonstrated that they can be readily produced by seeded suspension polymerization. Moreover, it is necessary to determine the influence of experimental parameters like expansion time, temperature and PMMA concentration on its expansion behavior and on the final expanded microstructure. This kind of information would be important when investigating the properties of molded plastic foams such as mechanical strength or chemical resistance. They would also be of interest to industrial engineers willing to obtain high performance polymeric foams.

The aim of this work is to evaluate the expansion of PS/PMMA core–shell particles and the effects of heating temperature, PMMA molar mass and PMMA amount in the shell on the expansion ratio and the evolution of the particle microstructure during the expansion.

EXPERIMENTAL

Materials

Technical grade methyl methacrylate (Rohm and Haas S.A., 99.6% purity) and styrene (Innova, 99% purity) were used as monomers. Benzoyl peroxide, *tert*-butyl peroxide and lauroyl peroxide (BPO, TBP and LPO, respectively, Sigma-Aldrich) were used as initiators. Distilled water was used as continuous phase and poly(vinyl pyrrolidone) (PVP, $M_w = 3.6 \times 10^5$ g mol^{-1}, Sul Polímeros) as stabilizer. Ascorbic acid (Sigma-Aldrich, 99.0% purity) was used to avoid inhibition caused by oxygen during the synthesis of the core-shell particles. *n*-pentane (Sigma-Aldrich) was used as blowing agent and silicon oil was used as heating medium in the particles expansion. All chemicals were used as received.

Core–Shell Synthesis

The reaction procedure to obtain the core–shell particles were presented in details elsewhere.[10] Briefly, Polystyrene (PS, $M_w = 1.80 \times 10^5$ g mol^{-1}) seeds were obtained by batch suspension polymerization using PVP at 1.0% w/w$_{water}$, BPO and TBP at 0.36% w/w$_{STY}$ and 0.1% w/w$_{STY}$, respectively. Polymerization was carried out for 6 h at 90°C followed by 2 h at 120°C to remove any trace of styrene monomer. PS beads retained between Tyler Standard sieves with nominal apertures of 710 and 1180 μm were used as seeds in the synthesis of the core–shell particles. The formulation employed is presented in Table I. The initial charge was composed by distilled water, polystyrene seeds, PVP and ascorbic acid. The monomer feed (0.9 g min^{-1}) was composed by MMA and initiator (LPO or BPO at the same molar concentration). In the first set of experiments, when lower amount of PMMA was incorporated to the PS seed particles, the monomer and the initiator were fed when the reactor was at the reaction temperature (70°C).

Table I. Formulation Used in All Core-Shell Synthesis Experiments

Reactant	Mass (g)
Water	560.000
Polystyrene seeds	197.400
Methyl methacrylate	62.000
Poly(vinyl pyrrolidone)	1.980
Ascorbic acid	0.789
BPO/LPO	0.341/0.561

After monomer feeding, the system was allowed to react for 4 h. In the second set of experiments, to increase the amount of PMMA incorporated, the monomer and the initiator were fed when the reactor was at 50°C and the system was kept at this temperature for an additional 40 min after monomer feeding. After that, the temperature of the reaction medium was increased to 70°C and the system allowed to react for 4 h. Benzoyl peroxide was used in all experiments except when stated.

Blowing Agent Incorporation

The core-shell particles were washed three times with distilled water to remove the adsorbed stabilizer (PVP) and then used in the blowing agent impregnation step. N-pentane was added at 10°C in the impregnation vessel to avoid its evaporation while all other compounds (listed in Table II) were added at room temperature. The vessel was tightly closed and the temperature was raised to 130°C. Then, after the desired time (2 or 4 h) has lapsed, the system was cooled. The particles were dried in a circulating oven at 30°C for 1 h and then stored at −10°C to prevent blowing agent loss.

Particles Expansion

A small amount of silicon oil was used as heating fluid. The silicon oil was placed in a Becker over a heating plate and its temperature was carefully controlled by a proportional-integral-derivative controller connected to the heating plate and to a thermocouple immersed in the oil bath. The expansion was recorded by a video camera and the particle diameter was measured using an image analysis software. For the morphology analysis the particles were immersed in the oil and then removed at the desired time. They were quenched in cold water and dried overnight.

Characterization

Expansion ratio (dimensionless) was calculated by eq. (1) where V_0 is the particle volume before expansion and V is the particle volume at a given expansion time.

$$\text{Expansion ratio} = \frac{V}{V_0} \tag{1}$$

Scanning Electron Microscopy (SEM, Philips XL-30 at 15 kV) was used to evaluate the expanded morphology. Particles were dried at 60°C in a forced air circulation oven and then cut in half with a laboratory razor blade at room temperature to expose the internal microstructure. Samples were coated with gold before analysis and the cell size distribution was determined from the SEM images using an image analysis software.

Table II. Formulation Used in the Blowing Agent Impregnation Step

Compounds	Mass (g)
Core-shell particles	3.000
Water	134.000
Poly(vinyl pyrrolidone)	1.340
n-pentane	0.300

Head-space gas chromatography (Shimadzu GC2010AF) was used to determine the *n*-pentane concentration in the core-shell particles and the equipment conditions were set as follows: Rtx-5 column (30 m × 0.25 mm, Restek), injector temperature at 250°C; nitrogen as carrier gas (flow rate of 1.39 mL min^{-1}); head space oven temperature of 50°C by 3 min; oven temperature initially at 50°C by 3 min and then raised to 190°C at 20°C min^{-1}.

Weight average molecular weight, M_w, was measured by size exclusion chromatography (SEC) using a Waters apparatus equipped with three Styragel columns in series (HR 2, HR 4, HR 6; effective molar mass ranges of $5 \times 10^2 - 2 \times 10^4$, $5 \times 10^3 - 6 \times 10^5$, and $2 \times 10^5 - 1 \times 10^7$ g mol^{-1}, respectively) at 35°C with tetrahydrofuran (THF) as eluent at 1.0 mL·min^{-1}. A Waters 2410 refractive index detector was used and molar masses were determined from a calibration curve based on PS standards from 580 to 1.12×10^7 g mol^{-1}. PMMA (shell polymer) was separated from PS (core polymer) before SEC analysis. This was implemented by dissolving a sample of the core–shell particles in THF for 12 h; after complete dissolution, cyclohexane was slowly added until PMMA precipitation occurred. The precipitate was separated by centrifugation and dried; after that, it was dissolved in acetic acid to separate any trace of polystyrene. The acetic acid soluble fraction was filtered and dried. Infrared spectra (Nicolet 5DXC) were obtained from the PMMA and PS fractions to ensure that each one was composed by pure polymer (peaks at 700 and 750 cm^{-1} were used to identify the presence of polystyrene, while the peak at 1740 cm^{-1} was used for PMMA). For all samples, IR spectra confirmed that the separation procedure was successful and that the polymer fractions were pure.

Glass transition temperatures of the pure polymers were determined by Differential Scanning Calorimetry (DSC, PerkinElmer STA 6000) under nitrogen at 30 mL min^{-1}. Samples were heated to 200°C at 10°C min^{-1} and kept for 30 min to eliminate their thermal history. Then, they were cooled to 0°C and heated to 200°C at 10°C min^{-1} to determine the glass transition temperature (T_g).

Core–shell particle composition was determined by Proton Nuclear Magnetic Resonance (^{1}H NMR) using deuterated chloroform as diluent at 20°C (Bruker Avance Spectrometer, 500 MHz). The PMMA molar percentage in the sample was determined by the peak of CH_3—O group (at 3.6 ppm) and the peaks characteristic of the aromatic ring of the polystyrene (between 7.2 and 6.2 ppm). The peaks of the CH_2 and CH groups were used to verify the integration error.

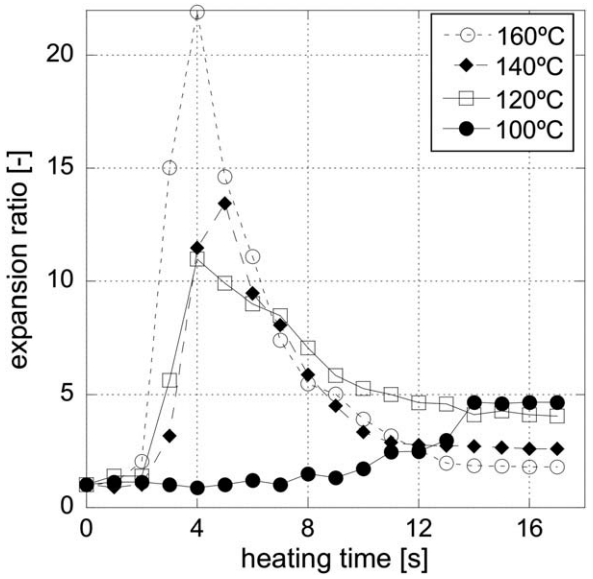

Figure 1. Effect of the temperature on the expansion of the core-shell particles (9 wt % PMMA; $M_w = 3.09 \times 10^6$ g mol^{-1}; 6 wt % *n*-pentane).

RESULTS AND DISCUSSION

Expansion Ratio

PS/PMMA core–shell particles (6 wt % *n*-pentane, impregnation time of 4 h) with distinct PMMA concentration and M_w were synthesized in order to evaluate their expansion ratio. The evaluation of the expansion ratio was carried out with PS/PMMA core-shell particles containing. This blowing agent concentration is similar to the one used in commercial expandable polystyrene and earlier results demonstrated that pure PMMA particles are able to expand with *n*-pentane concentrations of about 4 wt %.[23]

In the first set of experiments, described in the core–shell synthesis procedure, a concentration of 9 wt % of PMMA in the core–shell particles was obtained. When BPO was used as initiator, the weight average molecular weight of PMMA was equal to 3.09×10^6 g mol^{-1}. These particles were expanded at different temperatures as presented in Figure 1. At the temperatures of 120, 140, and 160°C (Figure 1) a maximum expansion ratio was observed and then expansion ratio decreased until it reached a plateau with increasing heating time. The higher the temperature, the higher the maximum expansion ratio, as increasing the temperature also increases the pressure exerted by the vapor of *n*-pentane in the polymer particle resulting in a larger volume of the cells. Besides that, the decrease in the viscosity of the melted polymer with increasing temperature reduces the resistance to the expansion process. The decrease in the expansion ratio for long heating times is explained by the collapsing of the cellular structure of the expanded polymer. Cell collapsing is caused by the drainage of polymer from the cell membrane into the cell ribs. As the cell walls are squeezed from a round shape into a polyhedral shape, a wall-thinning effect takes place, and polymer is drained from cell walls into the cell intersections.[29] This thinning effect can continue if the polymer is not cooled to a less mobile state leading to cell collapse and cell opening. The final expansion ratios decreased

Applied Polymer SCIENCE

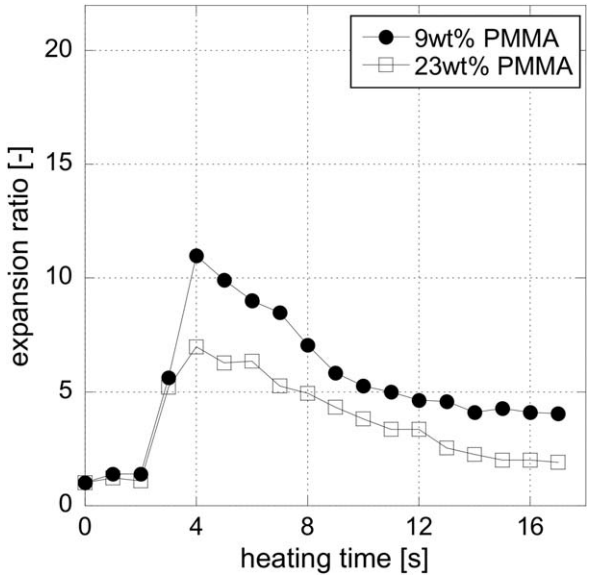

Figure 2. Effect of the amount of PMMA in the core-shell particles on the expansion of the core-shell particles ($M_w = 3.09 \times 10^6$ g mol^{-1}; expansion at 120°C; 6 wt % *n*-pentane).

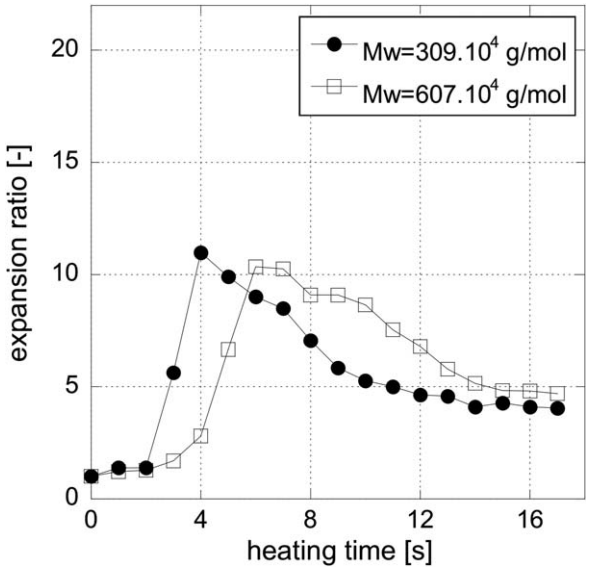

Figure 3. Effect of the PMMA molar mass on the expansion of the core-shell particles (9 wt % PMMA; expansion at 120°C; 6 wt % *n*-pentane).

with the increase in the temperature because cell collapse is more pronounced when the viscosity of the melted polymer is low.[29]

The core–shell particles presented a remarkable expansion when heated at 120°C and above this temperature, but at 100°C particles expanded only in a small extension. At 120°C and higher temperatures, expansion presented an induction period of 2 s after immersing the polymer bead in the hot silicon oil during which the temperature of the particle raised. The induction period observed was short since the particles were small enough to provide a high specific surface area resulting in a fast expansion. The expansion occurs when the temperature of the particle is higher than the boiling point of the blowing agent and the T_g of the polymer is reached. The *n*-pentane boiling temperature is low (36°C)[30] therefore, the resistance to the particle expansion at 100°C should be related to the T_g of the polymer. The glass transition temperature of the polymers without *n*-pentane is 99°C for PS ($M_w = 1.80 \times 10^5$ g mol^{-1}) and 120°C for PMMA ($M_w = 3.09 \times 10^6$ g mol^{-1}). Moreover, it is known that the presence of *n*-pentane lowers the polymer glass transition temperature. Preview results [23] showed that the presence of 4.5 wt % of *n*-pentane decreased the glass transition temperature of PMMA from approximately 119 to 88°C, which means that T_g falls by 6.9°C per wt% *n*-pentane which is a very similar value for that found for PS by around 7°C per wt % *n*-pentane. [13] It means that all expansion experiments were carried out at temperatures higher than the T_g of both polymers impregnated with 6 wt % of *n*-pentane including the expansion at 100°C. However, during the expansion *n*-pentane is released, therefore, the T_g of the polymer phase increased during the expansion and the PMMA-rich could had its T_g higher than the expansion temperature at 100°C.

The effect on the expansion ratio of the PMMA concentration (9 or 23 wt %) in the core–shell particles was evaluated at 120°C and is presented in Figure 2.

When the heating temperature is higher than the T_g of the polymer, expansion depends on the viscosity of the melted polymer because polymer must flow during the cell growth. Viscosity is mainly affected by molar mass and chain entanglement.[31–33] The molar mass of PMMA in the core-shell particles is far higher than its critical entanglement molar mass ($M_{c,PMMA} = 30 \times 10^3$ g mol^{-1})[34] which contributed to the increase of the viscosity in the PS/PMMA particles. The zero shear viscosities were measured by Carriere et al.[35] for melted PS (2.80×10^5 g mol^{-1}) and PMMA (26.9×10^3 g mol^{-1}) at different temperatures and showed that the zero shear viscosity at 140°C and 160°C was almost three times higher for PS, whereas PS had a M_w 10 times higher than PMMA . It is commonly accepted that the zero shear viscosity scale with the molecular weight as $(M_w)^{3.4}$ for monodisperse polymers with molecular weights substantially above the entanglement molecular weight.[36] In the expansion experiments, the M_w of PMMA (3.09×10^6 g mol^{-1}) was 17 times higher than the M_w of PS (1.80×10^5 g mol^{-1}) meaning that at the same temperature, the viscosity of the melted PMMA was expected to be much higher than the viscosity of the melted PS. This is in agreement with the fact that the increase in the PMMA amount also hindered the particles expansion in a greater extension (Figure 2) since particles containing 23 wt % PMMA presented half the expansion ratio when compared to those containing 9 wt % PMMA.

Figure 3 shows the expansion ratio of the core-shell particles with 9 wt % PMMA and different weight average molar masses, 3.09×10^6 g mol^{-1} (BPO as initiator) and 6.07×10^6 g mol^{-1} (LPO as initiator). The PMMA molar mass showed no remarkable influence on the maximum expansion ratio as demonstrated in Figure 3. However, particles with higher molar mass PMMA expanded only after an induction period of 4 s. This can be explained by the fact that the higher the polymer molar mass, the higher is the viscosity of the melted polymer which is valid for a wide variety of entangled linear polymers.[32,37] The increase in the viscosity

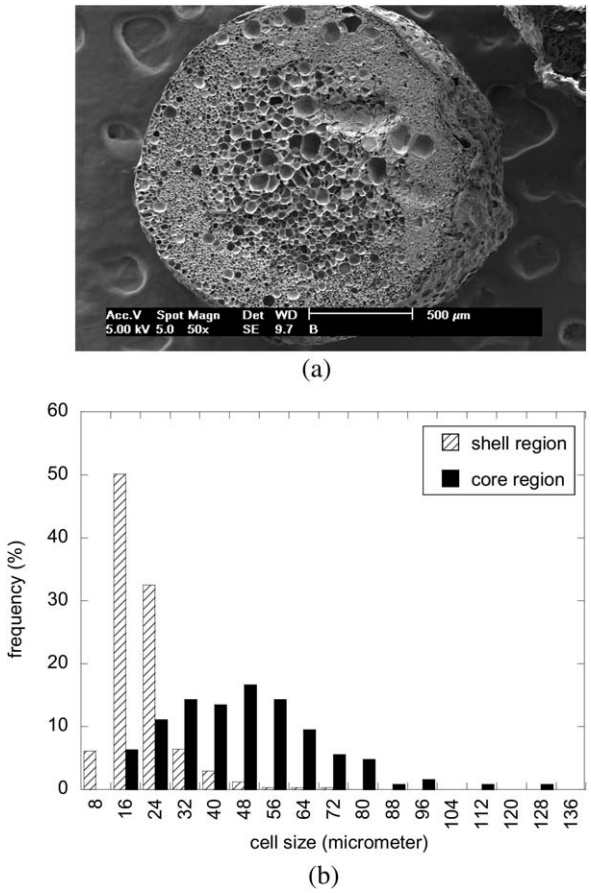

Figure 4. SEM images of the core-shell particles and cell size distribution (170°C, 20 s expansion; 9 wt % PMMA; 3 wt % *n*-pentane; $M_w = 3.09 \times 10^6$ g mol^{-1}; ×50). (a) Core–shell morphology. (b) Cell size distribution for the shell and core regions.

hindered cell growth at the earlier stages of the expansion process delaying the initial expansion.[13,29]

Particle Morphology after Expansion

Another set of experiments were carried out to obtain core–shell particles with a small amount of blowing agent. The objective was to obtain particles that could expand slower than those described above so that the evolution of the expanded microstructure could be better evaluated. The conditions used were the same described above but with an impregnation time of only 2 h resulting in a *n*-pentane concentration of 3 wt %. At this blowing agent concentration, the highest expansion ratio was observed when the particles were heated at 170°C, therefore, all the expansion experiments with 3 wt % of *n*-pentane were conducted at this temperature.

Figure 4(a) presents a low magnification SEM image of the microstructure of a core-shell particle expanded at 170°C during 20 s. The cellular microstructure was slightly damaged during the cut procedure as can be observed at the right side of the particle [Figure 4(a)], however it did not interfere with the analysis of the particle microstructure. The cell size distributions of the shell and core regions are presented in Figure 4(b). One can observe that the shell is composed by cells with an average size of 16 ± 1 μm while the center of the particle presented larger cells (44 ± 4 μm). The images confirmed that the core and shell structure still existed after the expansion and this kind of expanded structure is closely related to the particles synthesis conditions. In a previous work,[10] it was shown that the core–shell particles presented a polystyrene pure core and a shell composed by PMMA domains dispersed in a polystyrene continuous phase. Although bubble nucleation may occur due to discontinuities on local properties as density or molecular arrangement, the incompatibility between PMMA and PS could make the dispersed PMMA domains to operate as gathering sites for the blowing agent and as additional nucleation points during the blowing agent evaporation inside the particle. As one nucleation point generates one cell in a situation where no cell walls breakage takes place, increasing the number of nucleation points would increase the number of cells reducing the average size of the cells. This could explain the difference between the cell sizes in the core and the shell regions. It is also worth noting that the differences in the solubility of the blowing agent in each polymer could also influence the nucleation mechanism and thus the final expanded microstructure.

The particle morphology change during the expansion can be evaluated observing Figure 5 where (a), (c), (e), and (g) show the shell region while (b), (d), (f), and (h) show the core region at different expansion times.

The images (Figure 5) demonstrated that expansion was fast at 170°C and 3 wt % *n*-pentane since the cellular microstructure was fully formed after 3 s of heating and no major change was observed for increasing heating times.

To verify the effect of expansion temperature on the morphology and microstructure of the core–shell particles with a small amount of *n*-pentane (3 wt %), expansion experiments were carried out at different temperatures (120, 140, and 170°C) and samples were collected after 7 s of heating time. Figure 6 presents the internal microstructure of cut particles and Figure 7 presents the surface of the particles after heating.

At 120°C only the outer region of the particle was expanded presenting round cells formed by the evaporation of the blowing agent and no appreciable expansion could be seen in the center of the particle [Figure 6(a,b)]. At 140°C bubbles of the blowing agent were also formed in the center of the particle but they still presented round shape both in the shell and core regions.

The increase in the expansion temperature also led to cell rupture mainly observed at the particle surface (Figure 7), leading to the formation of channels throughout the particle. As described for the case of pure PMMA expandable particles[23] cell rupture is more pronounced at high temperatures because of the decrease of the viscosity of the melted polymer. According to Suh and Paquet,[29] cell rupture can be responsible for excessive moisture absorption, decrease in mechanical strength as well as the increase in thermal conductivity.

CONCLUSIONS

The expanded PS/PMMA particles presented a unique microstructure with the shell consisted of smaller polyhedral cells

Applied Polymer SCIENCE

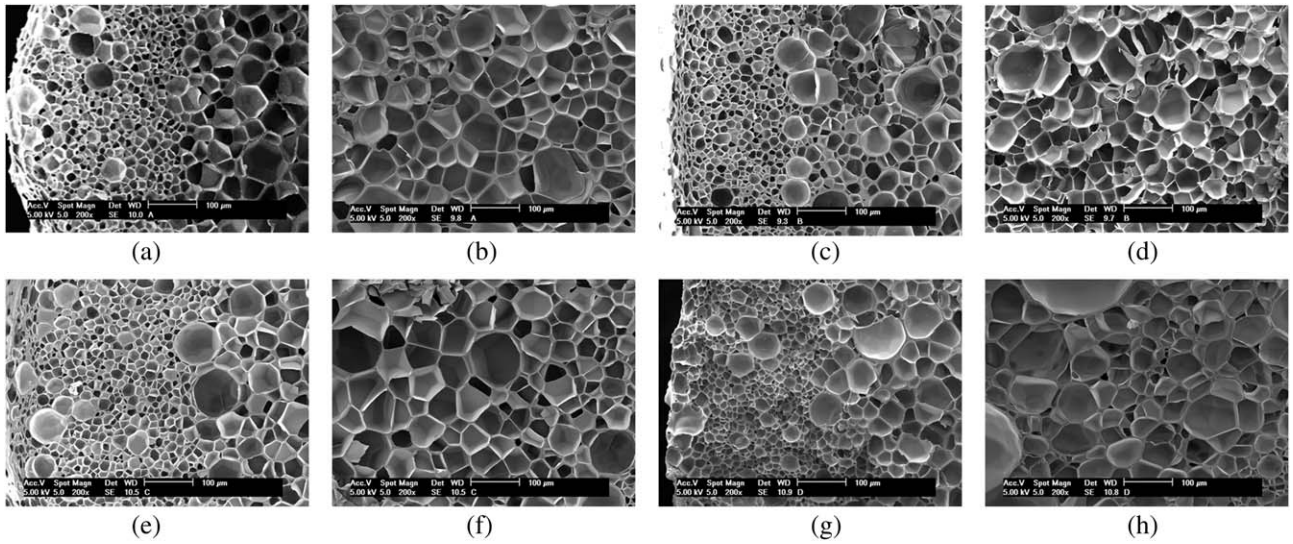

Figure 5. SEM images of the core–shell particles expanded at 170°C and different heating times (9 wt % PMMA; 3 wt % *n*-pentane; $M_w = 3.09 \times 10^6$ g mol^{-1}; ×200). (a) 3 s, shell region. (b) 3 s, core region. (c) 7 s, shell region. (d) 7 s, core region. (e) 15 s, shell region. (f) 15 s, core region. (g) 20 s, shell region. (h) 20 s, core region.

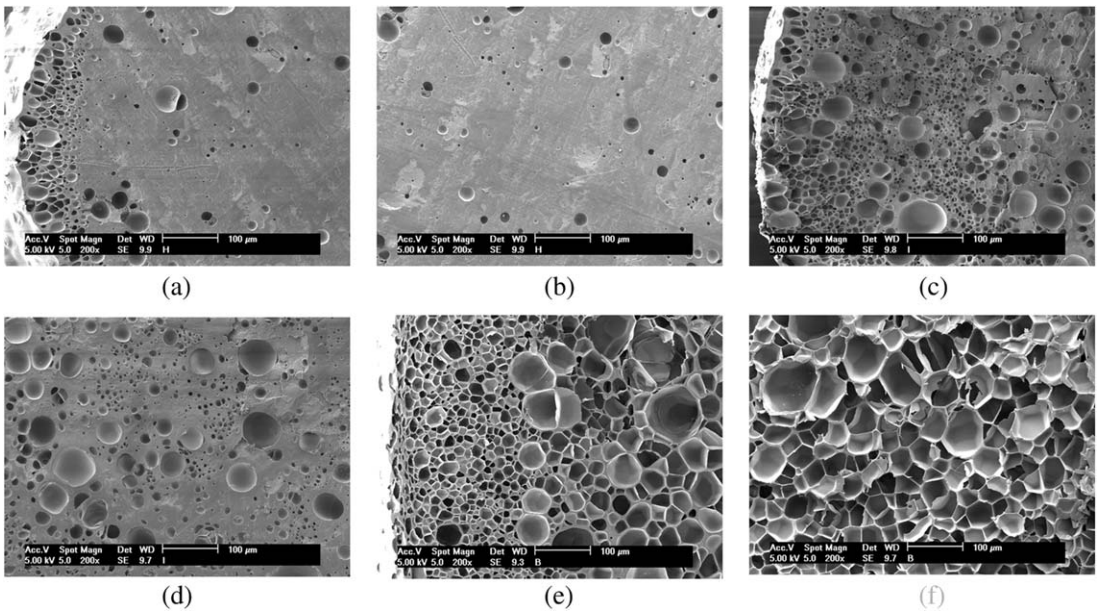

Figure 6. SEM images of the core–shell particles expanded at different temperatures (7 s heating time; 9 wt % PMMA; 3 wt % *n*-pentane; $M_w = 3.09 \times 10^6$ g mol^{-1}; ×200). (a) 120°C, shell region. (b) 120°C, core region. (c) 140°C, shell region. (d) 140°C, core region. (e) 170°C, shell region. (f) 170°C, core region.

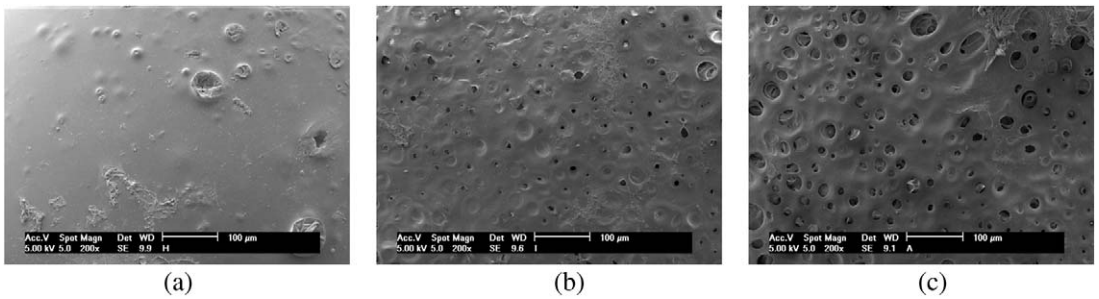

Figure 7. SEM images of the surface of the core-shell particles expanded at different temperatures (7 s heating time; 9 wt % PMMA; 3 wt % *n*-pentane; $M_w = 3.09 \times 10^6$ g mol^{-1}; ×200). (a) Expansion at 120°C. (b) Expansion at 140°C. (c) Expansion at 170°C.

while the center of the particle (core region) presented larger cells. Controlled expansion demonstrated that even low PMMA amounts in the shell significantly changed the expansion behavior of the particles. Core-shell particles containing 9 wt % PMMA and 6 wt % *n*-pentane had their volume increased up to 20 times depending of the heating temperature. The expansion ratio increased with increasing heating temperatures but higher amounts of PMMA hindered the expansion. Expansion ratio was not directly affected by the PMMA molar mass but a larger induction period was observed probably due to subsequent decrease in the polymer melt flow caused by the increased molar mass. During the expansion the morphology changed from round bubbles dispersed in the polymer matrix to polyhedral cells and cell wall rupture was observed mainly in the particle surface at higher heating temperatures.

ACKNOWLEDGMENTS

Laboratório Central de Microscopia Eletrônica, LCME - UFSC, is acknowledged for the SEM images. The authors are also grateful to Conselho Nacional de Desenvolvimento Científico e Tecnológico, CNPq, and Coordenação de Aperfeiçoamento de Pessoal de Nível Superior, CAPES, for the financial support.

REFERENCES

1. Schellenberg, J.; Wallis, M. *J. Cell. Plast.* **2010**, *46*, 209.
2. Bishop, R. B. Pratical Polymerization for Polystyrene; Cahners Publishing Co., Inc.: Massuchusetts, **1971**.
3. Lee, S-T. In Foam Extrusion Principles and Practice; Lee, S.-T., Ed.; CRC Press: Florida, **2000**.
4. Scheirs, J.; Priddy, D. B. In Modern Styrenic Polymers: Polystyrenes and Styrenic Copolymers; Scheirs, J.; Priddy, D. B., Eds.; Wiley: Chichester, **2003**.
5. Suh, K. W. In Handbook of Polymeric Foams and Foam Technology; Klempner, D.;Sendijarevic, V., Eds.; Hanser: Munich, **2004**.
6. Kitamori, Y. US Pat. 3,959,189, **1976**.
7. Kitamori, Y. US Pat. 4,168,353, **1979**.
8. Kajimura, M.; Kaisha, S. US Pat. 4,303,757, **1981**.
9. Kobayashi, S.; Nakamura, M. US Pat. 4,525,486, **1985**.
10. Gonçalves, O. H.; Asua, J. M.; Araújo, P. H. H.; Machado, R. A. F. *Macromolecules* **2008**, *41*, 6960.
11. Lin W.; Biegler, L. T.; Jacobson, A. M. *Chem. Eng. Sci.* **2010**, *65*, 4350.
12. Pontiff, T. In Foam Extrusion Principles and Practice; Lee, S.-T., Ed.; CRC Press: Florida, **2000**.
13. Klodt, R.; Gougeon, B. In Modern Styrenic Polymers: Polystyrenes and Styrenic Copolymers; Scheirs, J.; Priddy, D. B., Eds.; Wiley: Chichester, **2003**.
14. Munters, C. G.; Tandberg, J. G. US Pat. 2,023,204. **1935**.
15. Lintner, J.; Holl, K.; Petrovicki, H. CA Pat. 663,596. **1963**.
16. Morehouse Jr., D.S.; Tetreault, R. J. US Pat. 3,615,972. **1971**.
17. Han, C. D.; Kim, Y. W.; Malhotra, K. D. *J. Appl. Polym. Sci.* **1976**, *20*, 1583.
18. Han, C. D.; Villamizar, C. A. *Polym. Eng. Sci.* **1978**, *18*, 687.
19. Oyanagi, Y.; White, J. L. *J. Appl. Polym. Sci.* **1979**, *23*, 1013.
20. Brandrup, J.; Immergut, E. H.; Grulke, E. A. Polymer Handbook; Wiley-Interscience: New York, **1999**.
21. Adolph, V.; Wayne, P. US Pat. 4,652,609, **1987**.
22. Adolph, V.; Wayne, P. US Pat. 4,659,745, **1987**.
23. Gonçalves, O. H.; Staudt, T.; Araújo, P. H. H.; Machado, R. A. F. *Mater. Sci. Eng. C* **2009**, *29*, 479.
24. Gonçalves, O. H.; Nogueira, A. L.; Araujo, P. H. H.; Machado, R. A. F. *Ind. Eng. Chem. Res.* **2011**, *50*, 9116.
25. Mark, J. E. Polymer Data Handbook; Oxford University Press: New York, **1999**.
26. Jalili, K.; Abbasi, F.; Nasiri, M.; Ghasemi, M.; Haddadi, E. *J. Cell. Plast.* **2009**, *45*, 197.
27. Azimi, H. R.; Rezaei, M.; Abbasi, F. *J. Cell. Plast.* **2011**, *48*, 125.
28. Mehravar, E.; Abbasi, F.; Jalili, K.; Rezaei, M.; Heydarpoor, S. *J. Cell. Plast.* **2012**, *48*, 161.
29. Suh, K. W.; Paquet, A. N. In Modern Styrenic Polymers: Polystyrenes and Styrenic Copolymers; Scheirs, J.; Priddy, D. B., Eds.; Wiley: Chichester, **2003**.
30. Haynes, W. M., Ed.CRC Handbook of Chemistry and Physics, 92nd ed.; CRC Press/Taylor and Francis: Boca Raton, **2012**.
31. Fox, T. G.; Flory, P. J. *J. Am. Chem. Soc.* **1948**, *70*, 2384.
32. Colby, R. H.; Fetters, L. J.; Graessley, W. W. *Macromolecules* **1987**, *20*, 2226.
33. O'Connor, K. M.; Scholsky, K. M. *Polymer* **1989**, *30*, 461.
34. Graessley, W. W. In Advances in Polymer Science; Springer Verlag: New York, **1974**.
35. Carriere, C. J.; Biresaw, G.; Samler, R. L. *Rheol. Acta* **2000**, *39*, 476.
36. Nielsen, J. K.; Rasmussen, H. K.; Hassager, O.; McKinley, G. H. *J. Rheol.* **2006**, *50*, 453.
37. Bremner, T.; Rudin, A.; Cook, D. G. *J. Appl. Polym. Sci.* **1990**, *41*, 1617.